Determination of the Microscopic Equilibrium Dissociation Constants for Risedronate and Its Analogues Reveals Two Distinct Roles for the Nitrogen Atom in Nitrogen-Containing Bisphosphonate Drugs

Andrea M. Hounslow,[†] John Carran,[‡] Richard J. Brown,[†] Dominik Rejman,[‡] G. Michael Blackburn,[‡] and Donald J. Watts*[,†]

Department of Molecular Biology and Biotechnology, University of Sheffield, Firth Court, Western Bank, Sheffield S10 2TN, U.K., and Department of Chemistry, University of Sheffield, Dainton Building, Sheffield S3 7HF, U.K.

Received December 17, 2007

Microscopic equilibrium dissociation constants, k_as, were determined for four nitrogen-containing bisphosphonates (N-BP): risedronate and its analogues 2-(2-aminophenyl)-1-hydroxyethylidene-1,1-bisphosphonate, NE 11807, and NE 97220. The proportion of each and of analogues 2-(3′-(*N*-ethyl)pyridinium)-ethylidenebisphosphonate and 2-(3-piperinidyl)-1-hydroxyethylidene-1,1-bisphosphonate, having a positively charged nitrogen and three negative charges on the bisphosphonate group ("carbocation analogue") at pH 7.5, was calculated. When set in order of increasing potency at inhibiting farnesyl diphosphate (FDP) synthase (their intracellular target), the N-BPs are also ranked in order of decreasing mole fraction of carbocation analogue. However, only a weak correlation exists between potency for inhibiting FDP synthase and potency for inhibiting *Dictyostelium discoideum* growth. It is concluded that, although high potency for inhibiting FDP synthase is favored when the nitrogen atom in a N-BP is uncharged, N-BPs having a positively charged nitrogen can still be potent inhibitors of *Dictyostelium* growth owing to favorable interaction with a second, unidentified target.

Introduction

Risedronate and alendronate (Figure 1) are the antiresorptive N-BP[a] drugs most widely used to treat osteoporosis owing to their particularly high potency at inhibiting osteoclast-mediated bone resorption.[1,2] They also inhibit growth of the amoeboid microorganism *Dictyostelium discoideum*,[3,4] and investigations making use of this model system were the first to identify the intracellular target for the drugs as the enzyme farnesyl diphosphate synthase.[5] However, the characteristic nitrogen atom of the N-BPs is essential to their high potency at inhibiting both bone resorption and growth of *Dictyostelium*,[3,4,6,7] yet neither the substrates nor the products of the reaction catalyzed by FDP synthase contain a nitrogen atom. It was therefore proposed[5,8] that the N-BPs might be acting as analogues of the carbocation transition state of the enzyme-catalyzed reaction.[9] This would be possible only when the nitrogen atom in an N-BP is positively charged at physiological pH, and this condition is met in alendronate and some other N-BPs. It was less clear that the nitrogen atom in risedronate would be positively charged at physiological pH because it is in a pyridine ring and pyridines generally have pK_a values below 7. It was therefore important to determine the proportion of risedronate that exists as the carbocation analogue at physiological pH (ca. pH 7−7.5) to gain further insight into the mechanism of action of the N-BP drugs.

In addition to the positively charged nitrogen atom, the carbocation analogue must possess a bisphosphonate group carrying three negative charges because this is essential for strong binding to FDP synthase.[10,11] It also proved valuable to determine for some risedronate analogues (Figure 1) the proportion of the carbocation analogue present at physiological pH.

Methods

Determination of pK_a Values by Potentiometric Titration. In general, N-BPs are pentaprotic acids, but after dissolution, they may be treated as tetraprotic or triprotic acids. Titration of a tetraprotic weak acid H_4L with a strong base (e.g., KOH) involves eight solution species: H_3O^+, OH^-, H_4L, H_3L^-, H_2L^{2-}, HL^{3-}, L^{4-}, and the metal cation, K^+. Other variables are the initial acid concentration (A_{init}), the initial base concentration (B_{init}), volume of acid titrated (V_a), and the volume of base added (V_b). The algebraic description of a tetraprotic titration (neglecting activities) is completely specified by four equations for the four ionization steps (K_a1, K_a2, K_a3, and K_a4), the equation for ionization of water (K_w), equations for the mass and charge balance, and, in addition, two equations to account for dilution of the acid and base concentrations during the titration. Solving for V_b by use of an algebra program (Mathematica) yields an expression for the volume of base V_b as a function of pH, the four K_a values, K_w, the volume of acid V_a, and the initial concentrations of acid and base A_{init} and B_{init}. Nonlinear regression performed on the data from the potentiometric titrations of N-BPs and the deaza-analogue of risedronate (**1**) gave values of pK_a3 and pK_a4 (Table 1).

Determination of Microscopic Equilibrium Dissociation Constants, k_as. NMR−pH titrations have been used extensively to determine macroscopic dissociation constants for polyprotic systems in which the dissociation steps are well separated ($\Delta pK_a = (pK_{a,i+1} - pK_{a,i}) > 3$). If the dissociation steps are overlapping, the p$K_{a,i}$ values describe the stoichiometry but not the site of protonation as there are intermediate species that have the same number of protons but at different protonation sites. The microspecies cannot be separated analytically, but in favorable circumstances, the mole fraction of one species may

* To whom correspondence should be addressed. Tel.: +44 114 222 4196, Fax: +44 114 222 2800. E-mail: d.j.watts@sheffield.ac.uk.
[†] Department of Molecular Biology and Biotechnology.
[‡] Department of Chemistry.

[a] Abbreviations: N-BP, nitrogen-containing bisphosphonate; FDP, farnesyl diphosphate; ND, not determined; DSS, 2,2-dimethyl-2-silapentane-5-sulfonate, sodium salt.

10.1021/jm7015792 CCC: $40.75
Published on Web 07/01/2008

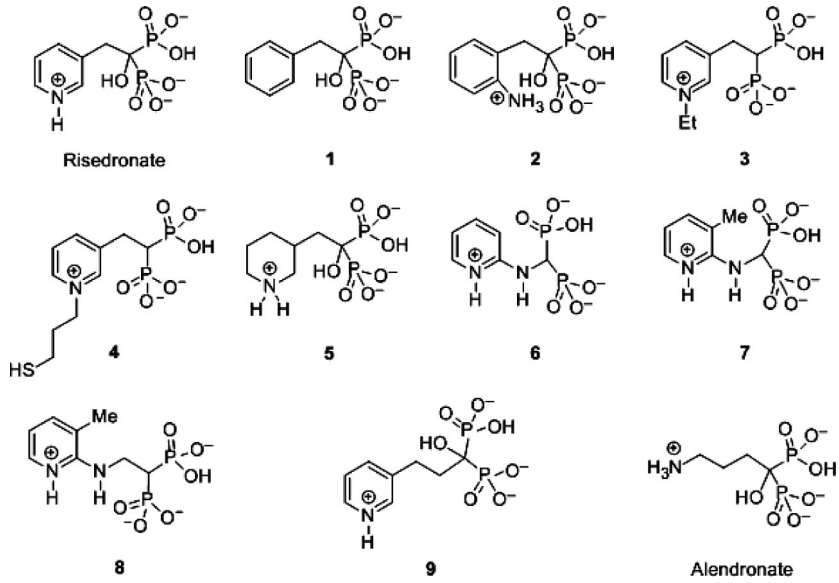

Figure 1. Chemical structures of risedronate, its analogues, and alendronate shown (except for **1**) in the "carbocation analogue" form.

Table 1. Values of pK_as, Determined by Potentiometric Titration in the Range pH 2−12 for Some Nitrogen-Containing Bisphosphonates and 1-Hydroxy-2-(phenyl)-ethane-1,1-bisphosphonate (**1**)

bisphosphonate	pK_a3	pK_a4
risedronate	5.54	6.83
2	5.06	6.85
4	6.48	≥10
1	6.48	≥10
6	5.46	7.73
7	5.48	8.40
8	5.92	8.48
9	5.74	6.82
alendronate	6.17	≥10

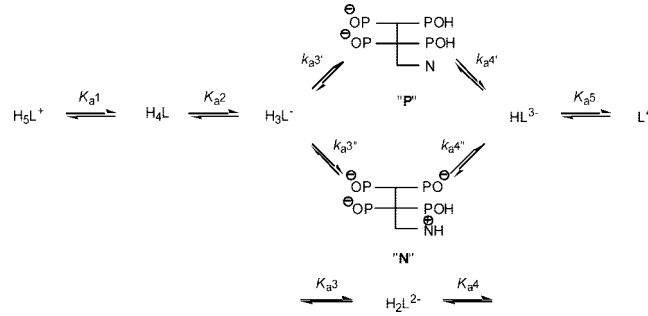

Figure 2. Dissociation of nitrogen-containing bisphosphonates.

be determined by NMR spectroscopy if the protonation of the "other" site(s) has no effect on the chemical shift of a "marker" nucleus.[12]

For the dissociation scheme shown in Figure 2, the observed pH-sensitive chemical shift of any protonation-sensitive nucleus can be given by

$$\delta^{\mathrm{obs}} = \frac{\delta_{\mathrm{L}^{4-}}[\mathrm{L}^{4-}] + \delta_{\mathrm{HL}^{3-}}[\mathrm{HL}^{3-}] + \delta_{\mathrm{H_2L}^{2-}}[\mathrm{H_2L}^{2-}] + \cdots + \delta_{\mathrm{H_5L}^{+}}[\mathrm{H_5L}^{+}]}{[\mathrm{L}^{4-}] + [\mathrm{HL}^{3-}] + [\mathrm{H_2L}^{2-}] + \cdots + [\mathrm{H_5L}^{+}]}$$

$$= \frac{\delta_{\mathrm{L}^{4-}} + \delta_{\mathrm{HL}^{3-}}10^{-\mathrm{p}\beta_1-\mathrm{pH}} + \delta_{\mathrm{H_2L}^{2-}}10^{-\mathrm{p}\beta_2-2\mathrm{pH}} \cdots + \delta_{\mathrm{H_5L}^{+}}10^{-\mathrm{p}\beta_5-5\mathrm{pH}}}{1 + 10^{-\mathrm{p}\beta_1-\mathrm{pH}} + 10^{-\mathrm{p}\beta_2-2\mathrm{pH}} + \cdots + 10^{-\mathrm{p}\beta_5-5\mathrm{pH}}} \quad (1)$$

where the β_i are so-called cumulative macroscopic constants related to the individual K_a values by

$$\beta_i = \frac{[\mathrm{H}_i\mathrm{L}^{(4-i)-}]}{[\mathrm{L}^{4-}][\mathrm{H}^+]^i} = \prod_{j=6-i}^{5} K_{a,j}^{-1} \quad (2)$$

Combining eqs 1 and 2 gives an expression relating observed chemical shift to pH as a function of the K_as and the chemical shifts of each of the protonation states. The NMR−pH titration curve for each protonated ^{13}C nucleus and its associated ^{1}H was fitted using nonlinear regression to the relevant equation over the pH range for the NMR titration. As this involved four pK_as and five chemical shifts, the equation was simplified by fixing pK_a2 and pK_a5 at 2.8 and 10.45, respectively,[13] for risedronate and solving for the two pK_as relevant to this study. Similarly, pK_a2 was set to 2.0 for **6** and **7**, and the equation was solved for three pK_as and five chemical shifts. The pK_as for the molecule were obtained by taking the average of the values of pK_a3, pK_a4, or pK_a5 determined from data for each nucleus.

The macroscopic pK_as and chemical shifts for the macrospecies were deconvoluted into microconstants by determining the site-specific protonation mole fraction. This can be achieved by assuming that the chemical shift of a nucleus i in the H_2L^{2-} species differs from that in HL^{3-} only as a consequence of protonation of the **N** site and not of the **P** site (Figure 2).

Defining the mole fraction of the N-protonated species as

$$x_{\mathrm{N}} = \frac{[\mathbf{N}]}{[\mathbf{N}] + [\mathbf{P}]} \quad (3)$$

then, because the microspecies are in fast exchange on the NMR time scale, the observed chemical shift of nucleus i in H_2L^{2-} is given by

$$\delta_{i,\mathrm{H_2L}^{2-}} = x_{\mathbf{N}}\delta_{i,\mathbf{N}} + (1 - x_{\mathbf{N}})\delta_{i,\mathbf{P}} \quad (4)$$

where $\delta_{i,\mathbf{N}}$ and $\delta_{i,\mathbf{P}}$ are the chemical shifts of nucleus i in the **N** and **P** species, respectively. Given the above assumption, then

$$\delta_{i,\mathbf{N}} = \delta_{i,\mathrm{H_3L}^{-}} \quad (5)$$

$$\delta_{i,\mathbf{P}} = \delta_{i,\mathrm{HL}^{3-}} \quad (6)$$

that is, the chemical shift of nucleus i in species **N** is the same as that of the protonated species, H_3L^- and the chemical shift in species **P** is the same as the deprotonated species, HL^{3-}.

Combining eqs 3−6 gives

$$x_{\mathbf{N}} = \frac{\delta_{i,\mathrm{H_2L^{2-}}} - \delta_{i,\mathrm{HL^{3-}}}}{\delta_{i,\mathrm{H_3L^{-}}} - \delta_{i,\mathrm{HL^{3-}}}} \quad (7)$$

From the fitted values of the macroscopic pK_as and the calculated value of $x_{\mathbf{N}}$, the microscopic pk_as and the distribution of each of the species as a function of pH were determined as described by Szakács et al.[14]

Calculation of the Proportions of Ionic Species from Spectrophotometric Measurements. The N-BPs exist as ionic species in which the nitrogen either is uncharged (**n** species) or is protonated and positively charged ($\mathbf{n}^+$ species). Provided that there is a wavelength at which the **n** species has a significantly different molar absorptivity from that of the $\mathbf{n}^+$ species, spectrophotometry may be used to determine the proportion of the N-BP existing as either of the two species at any pH.

If the proportion of the **n** species is α and the proportion of the $\mathbf{n}^+$ species is β and the microscopic and macroscopic equilibrium dissociation constants are as shown in Figure 2,

$$\alpha = \frac{k_a3'[\mathrm{H^+}] + K_a3K_a4}{[\mathrm{H^+}]^2 + K_a3[\mathrm{H^+}] + K_a3K_a4}$$

and

$$\beta = \frac{k_a3''[\mathrm{H^+}] + [\mathrm{H^+}]^2}{[\mathrm{H^+}]^2 + K_a3[\mathrm{H^+}] + K_a3K_a4}$$

The values of k_a3' and k_a3'' may then be obtained, for example, by use of non-linear regression analysis. Since, also,

$$K_a3 \cdot K_a4 = k_a3' \cdot k_a4' = k_a3'' \cdot k_a4''$$

the values of k_a4' and k_a4'' may be calculated.

Results and Discussion

Dissociation of Risedronate. Potentiometric titration of risedronate (Figure 3) shows that two protons dissociate from this N-BP between pH 4 and pH 9. The overlapping macroscopic pK_as were determined by deconvolution analysis of the titration curves, and the values of the pK_a were 5.54 and 6.83 (Table 1) with the quality of r^2 for the curve fit better than 0.9997.

The close proximity of the two pK_a values indicated that dissociation of risedronate follows the pathways shown in Figure 2. It is not usually possible to measure directly the concentration of any of the ionic species on alternative pathways for dissociation but the proportion of any species present at a selected pH may be calculated provided that the values of the microscopic equilibrium dissociation constants, k_as, for inter-

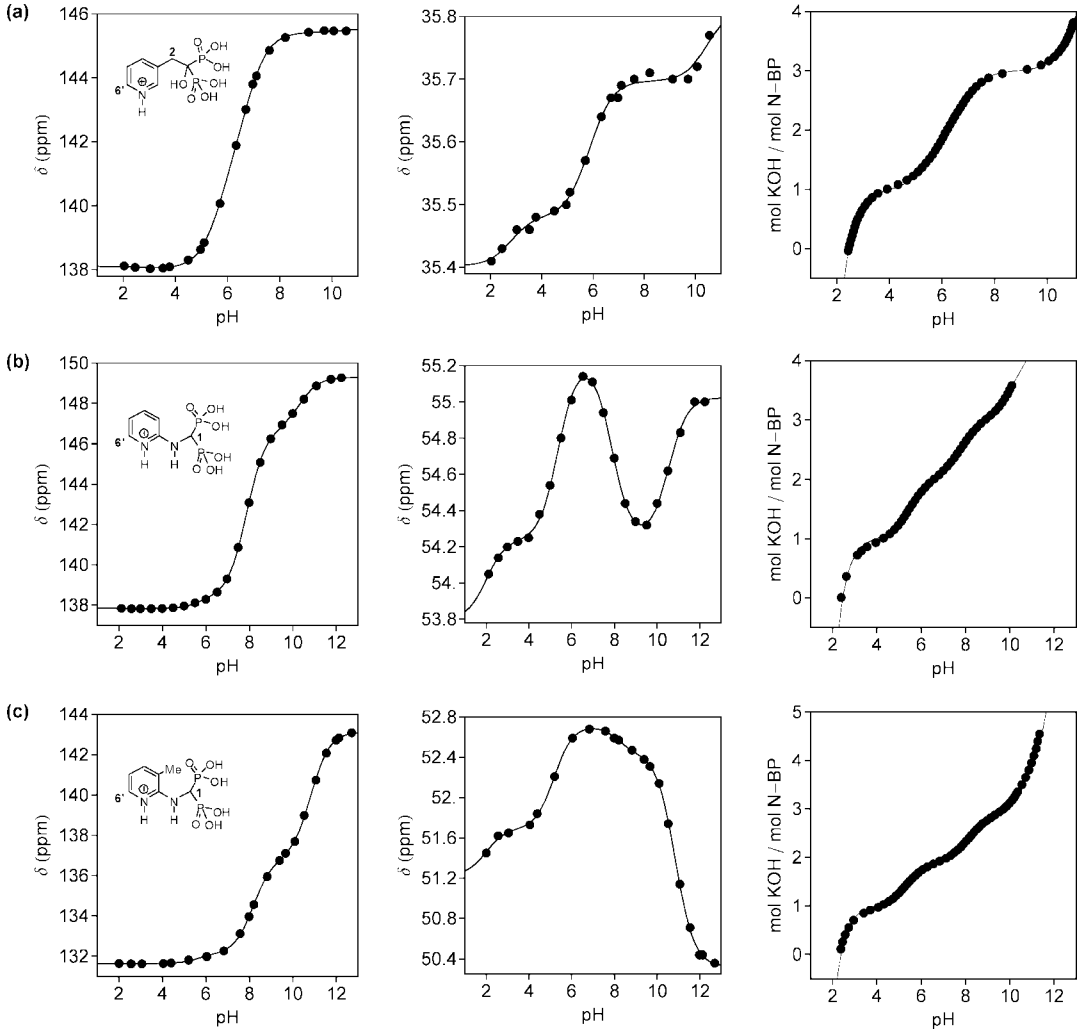

Figure 3. Titration of nitrogen-containing bisphosphonates. The pH dependence of ^{13}C NMR chemical shifts for (a) C-6′ (left) and C-2 (center) for risedronate, (b) C-6′ (left) and C-1 (center) for **6**, and (c) C-6′ (left) and C-1 (center) for **7**. Potentiometric titration curves for (a) risedronate, (b) **6**, and (c) **7**, are on the right. It should be noted that, at extremes of pH (below pH 2.5 and above pH 10.5), the potentiometric titration curve largely represents titration of water. The lines correspond to the equations in the text and Supporting Information with parameters determined by non-linear regression.

Table 2. Values for Macroscopic pK_as and Microscopic pk_as, Determined by NMR−pH Titration in the Range pH 2−12 for Risedronate and Nitrogen-Containing Bisphosphonates **6** and **7** and by UV Spectrophotometry for Nitrogen-Containing Bisphosphonate **2**[a]

bisphosphonate	pK_a3	pK_a4	pK_a5	pk_a3′	pk_a3″	pk_a4′	pk_a4″	pk_a3′ − pk_a3″
risedronate	5.66	6.74		6.00	5.92	6.40	6.48	0.08
2	5.06	6.85		5.44	5.29	6.47	6.62	0.15
6	5.52	7.84	10.22	6.66	5.55	6.69	7.81	1.11
7	5.38	8.16	10.82	6.40	5.42	7.13	8.11	0.98

[a] Error in pK_a values is estimated at ±0.05, with a reproducibility of ±0.02, arising primarily from the accuracy of pH meter calibration.

conversion of the ionic species can be determined. This was possible for risedronate after the proportions of this N-BP that were in all ionic forms containing a pyridinium ring between pH 2, when all of the risedronate is in the pyridinium form, and pH 12, when none of the risedronate is in the pyridinium form, had been determined by spectrophotometry (the pyridinium ring in risedronate has a larger molar absorptivity than the pyridine ring at 262 nm).

In addition, the microscopic k_as could be obtained after the proportion of the diprotonated species H_2L^{2-} containing a pyridinium ring had been determined by use of ^{13}C NMR spectroscopy. This method depends on the assumption that the chemical shift of C-6′ of the pyridinium ring (Figure 3) is affected only by dissociation of the proton from the adjacent N-1′ and not by a third dissociation from the bisphosphonate group. Because the change in chemical shift for C-6′ over the entire pH range was the same as that observed for pyridine,[15] this assumption must be valid. Furthermore, the close correlation between pk_as obtained by NMR spectroscopy and by spectrophotometry (not shown) also demonstrated that this assumption is justified.

The microscopic equilibrium dissociation constants obtained by NMR spectroscopy, which was inherently more accurate experimentally than spectrophotometry for investigations of risedronate, are given in Table 2, and the calculated proportions of risedronate in each ionic form between pH 1 and pH 13 are shown in Figure 4.

Dissociation of Nitrogen-Containing Bisphosphonate 2. The macroscopic pK_a values obtained for 2-(2-aminophenyl)-1-hydroxyethylidene-1,1-bisphosphonate **2** by deconvolution of the potentiometric titration curve (Table 1) indicated that this N-BP dissociates in a manner similar to that for risedronate. Only the ionic forms of **2** that contain an uncharged amino group absorb ultraviolet light at 283 nm, and it was therefore convenient to use spectrophotometry to determine the proportion of **2** in these ionic forms between pH 2 and pH 10 (because the use of NMR was problematic owing to the low solubility of **2**). Following calculation of the microscopic equilibrium dissociation constants (Table 2), the proportions of **2** in each ionic form between pH 1 and pH 13 were calculated (Figure 4).

Dissociation of Nitrogen-Containing Bisphosphonates 6, 7, and 8. Potentiometric titration curves obtained for **6**, **7**, and **8** showed that for each N-BP there are two well-separated proton dissociations between pH 4 and pH 9 and their macroscopic pK_a values are given in Table 1. Values for macroscopic pK_a5 (Table 2) were also obtained for **6** and **7** when titration with KOH at high pH was monitored by use of ^{13}C NMR.

Nitrogen-containing bisphosphonate **7** is a derivative of 2-amino-3-methylpyridine for which[16] the pK_a is 7.24. This clearly indicates that the macroscopic pK_a of **7** at 8.40 (Table 1) arises largely from dissociation of the pyridinium group. The pK_a for **7** at 5.48 was attributed largely to dissociation of the third proton from the bisphosphonate group because the positive charge in the 2-aminopyridine will have the effect of markedly reducing the bisphosphonate group pK_a3 (compare the pK_as for dissociation of the carboxyl groups of nicotinic acid [2.00] and benzoic acid [4.20][17] or the values of pK_a3 for pamidronate [6.04] and etidronate [6.87][18]). Attribution of pK_a3 to the bisphosphonate group and pK_a4 to the nitrogen group is different from that presumed elsewhere[19,20] but is supported by data (Figure 3) obtained when ^{13}C NMR was used to monitor titration

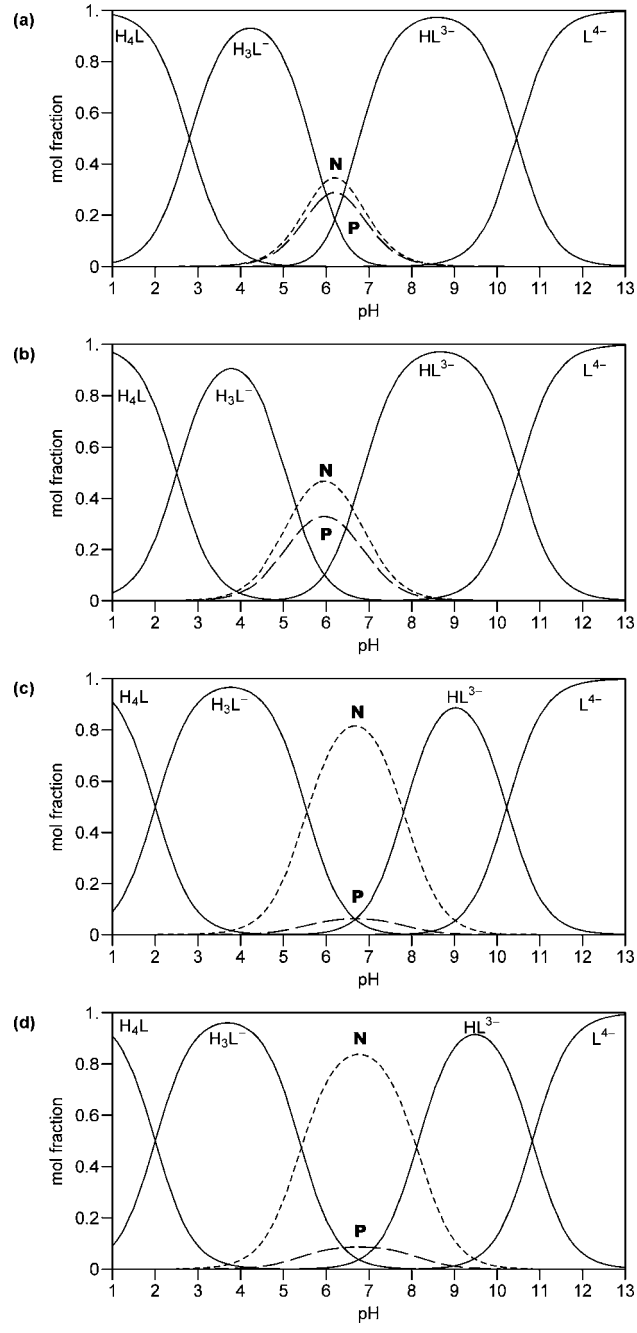

Figure 4. Speciation curves calculated from the pK_a and pk_a values in Table 2. (a) Risedronate, (b) **2**, (c) **6**, and (d) **7**. Species are identified according to the dissociation scheme in Figure 2, where **N** is the "carbocation analogue" species and **P** is the dianionic species with an uncharged nitrogen.

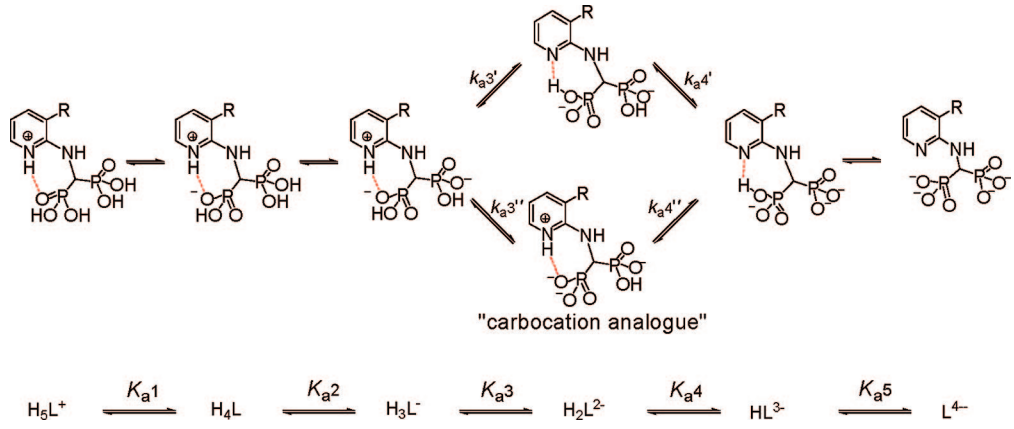

Figure 5. Dissociation pathways for **6** and **7** showing proposed H-bonding to nitrogen (red). R = H for **6**, R = Me for **7**.

Table 3. Inhibition of Farnesyl Diphosphate Synthase and Growth of *Dictyostelium* by Risedronate, Risedronate Analogues, and Alendronate

	inhibition of FDP synthase			
bisphosphonate	concentration (nM)	inhibition[a] %	proportion as the carbocation analogue at pH 7.5 (%)	IC_{50} for inhibition of *Dictyostelium* growth (μM)
1	200	53 ± 0.3	0	>180, < 240
risedronate	2	57 ± 1.0	8	13[b]
2	7	63 ± 0.8	11	18
6	8	63 ± 1.5	63	12[b]
7	10	55 ± 3.5	74	9[b]
3	35	59 ± 3.0	>90	27
5	30	58 ± 2.0	>90	30
9	100	23[c]	ND	310[b]
8	200	32 ± 3.1	ND	40[b]
alendronate	100	44 ± 2.0	>90	32[b]

[a] Results are given as the mean ± SEM for three independent observations. [b] Data taken from ref 4. [c] Calculated from data in ref 5.

of **7** with KOH. In the range pH 3−6.5, there is a marked change in the chemical shift of C-1 but very little change in the chemical shift of C-6′, indicating that dissociation of a proton in this pH range is essentially from the bisphosphonate group and not from the pyridinium group. There are also changes in the chemical shifts of C-1 and C-6′ between pH 7 and 9.5 and again between pH 9.5 and 12 (Figure 3) indicating that dissociation of a proton from either the pyridinium group or the bisphosphonate group affects the chemical shifts of carbon atoms in both the aromatic ring and the bisphosphonate group owing to hydrogen bonding (Figure 5).

Although **7** dissociates predominantly by loss of a proton from the bisphosphonate group followed by loss of a proton from the pyridinium group as the pH rises above pH 4, protons will dissociate from a very small proportion of **7** in the opposite sequence (Figure 5). From the ^{13}C NMR profiles (Figure 3), it was possible to calculate the microscopic equilibrium dissociation constants, k_as, (Table 2) and hence the proportions of each ionic species present on the alternative pathways of dissociation over the range pH 1−13 (Figure 4).

The microscopic equilibrium dissociation constants, k_as, for **6** were calculated similarly (Table 2), and the proportions of **6** in all of its ionic species between pH 1 and pH 13 were determined (Figure 4).

Inhibition of Farnesyl Diphosphate Synthase and Inhibition of Growth of *Dictyostelium discoideum*. Concentrations of risedronate and of its analogues that caused approximately 50% inhibition of FDP synthase at pH 7.5 were determined, and these allowed the potencies of the N-BPs as inhibitors of FDP synthase to be set in rank order. Risedronate is more potent than any of its analogues as an inhibitor of the synthase (Table 3), although some of the risedronate analogues are at least as potent as risedronate as inhibitors of growth of *Dictyostelium* (Table 3). The risedronate analogue **1** is a comparatively poor inhibitor of both FDP synthase and of *Dictyostelium* growth although the effect of this deaza-analogue on *Dictyostelium*-growth varied from experiment to experiment and there appeared to be no unique value for IC_{50}. The range of concentration in which the values of IC_{50} fall has therefore been given in Table 3.

General Discussion

Population of Protonic States. A prime requirement for understanding the role of the nitrogen function in a range of N-BP drugs is an accurate knowledge of the relative population of the various protonation states at physiological pH. The N-BPs are polyprotic acids, having four ionizable P-OH groups and one ionizable cationic N−H group. Because polyprotic acids with N titratable groups have $(2^N - 1)$ independent microscopic constants,[21] the complete resolution of the 31 microscopic pk_as for the N-BPs is a task virtually beyond experimental resolution. However, the problem can be simplified by focusing attention on only those functions that manifest reversible deprotonation in the pH range 4−10. Pentaprotic N-BPs have values for macroscopic pK_a1 and pK_a2 in the region of 1.0 and 2.0, respectively and pK_a5 above 10.5, corresponding to the first, second, and fourth ionizations of the four P-OH groups. Thus, the important ionization constants in the physiological pH range are macroscopic pK_a3 and pK_a4 and the four microscopic pk_as associated with loss of the third and fourth protons from the pentaprotic acids. These constants result from ionization, in unknown order, of the third P-OH and the N−H function.

Usually, determination of microscopic pk_as is initiated by potentiometric titration to identify the macroscopic pK_as. This

requires a curve-fitting analysis in the case of multiple protonation sites that titrate in the same pH range. The reliability of this derivation of the pK_as can be seen by the very high values for r^2 obtained with the curve-fitting program employed.

In order then to determine the microscopic pk_a values, titration curves are needed for an individual ionizing group that dissociates over the requisite pH range. These are most frequently obtained by NMR spectroscopy. The principle here is that sensor nuclei (^{13}C, ^{31}P, non-exchangeable ^{1}H) in the vicinity of an ionizing group are assumed to monitor the site-specific ionization.[12] Largely as a result of considering spatial effects and through-bond signal responsivity, we identified C-6′ (adjacent to the pyridine nitrogen and most distant from the bisphosphonate group) as the optimum nucleus for monitoring ionization of the N−H proton in the N-BPs (Figure 3 left column and Supporting Information).

The titration curves obtained by ^{1}H and ^{13}C NMR spectroscopy were also used to determine the values of the macroscopic pK_as (Figure 3 and Supporting Information) for each N-BP. Use of NMR spectroscopy also has the advantage that macroscopic pK_as can be determined that fall in a pH range where data obtained by potentiometric titration may be unreliable (e.g., above pH 10). General agreement was found between the macroscopic pK_a values obtained by potentiometric titration and by NMR spectroscopy (Tables 1 and 2), although they were obtained in slightly different conditions, the samples for NMR spectroscopy containing 10% D_2O.

Although these analyses (Table 2) may not have achieved overall the full physical chemistry rigor of a thermodynamic, multisite derivation of macroscopic, microscopic, and quasisite pK_a values,[21] we believe that they do provide a more accurate definition of the situation for N-BPs than has been achieved hitherto.[22]

The speciation curves (Figure 4) identify the mole fraction of the carbocation analogue (species **N**) as a function of pH. It is clear that for all four N-BPs, the **N** form of the dianion, H_2L^{2-}, preponderates over the nonzwitterionic **P** form and that the magnitude of this preponderance is directly related to the difference pk_a3' − pk_a3'' (i.e., the difference between the microscopic pk_as for dissociation of the third proton from the N-BPs) (Table 2).

Nitrogen-Containing Bisphosphonates and Inhibition of Farnesyl Diphosphate Synthase. Following our original identification of FDP synthase as the intracellular target for the N-BPs,[5] it has been generally assumed that the characteristic nitrogen atom of the N-BPs must play an essential role in the inhibition of this enzyme. This has been confirmed in the case of risedronate because its deaza-analogue **1** has a 100-fold decreased potency as an inhibitor of FDP synthase (Table 3).

Previously, it was found[5] that risedronate was the most potent FDP synthase inhibitor when compared with other commonly studied N-BPs. Furthermore, it has also been shown to be more potent than any of its analogues at inhibiting the synthase (Table 3). At pH 7.5, the pH at which inhibition of FDP synthase was determined, it is apparent that risedronate exists largely as the trianion and that only a little (about 8%) is present in the **N**, carbocation, form (Figure 4a). Likewise, **2**, the N-BP nearest in potency to risedronate as an inhibitor of FDP synthase (Table 3), also exists as the carbocation analogue to only a minor extent (about 11%) at pH 7.5 (Figure 4b). Values of pK_a3 for 2-(3′-(*N*-ethyl)pyridinium)-ethylidenebisphosphonate **3** and 2-(3-piperinidyl)-1-hydroxyethylidene-1,1-bisphosphonate **5** were not available directly,[23] so pK_a3 values in the range 6.17−6.48 were adopted because of the close structural resemblance of **3** and **5** to **4** and alendronate, respectively (Table 1). These pK_as indicate that, at pH 7.5, more than 90% of **3** and **5** will be present as **N**, the carbocation analogue, and both of these risedronate analogues have low potency at inhibiting FDP synthase (Table 3). Moreover, **6** and **7**, although less potent than risedronate as FDP synthase inhibitors, are more potent than **3** and **5**, and it was also found that **6** and **7** exist at pH 7.5 in proportions of the carbocation analogue, **N**, that are greater than for risedronate but less than for **3** and **5** (Table 3, Figure 4c,d). When, therefore, the overall effects of risedronate and its analogues are compared, there is a general, yet significant, correlation between an *increased* mole fraction of **N**, the carbocation analogue, at pH 7.5 and a *decreased* potency at inhibiting FDP synthase. This observation, that most potent inhibition of FDP synthase is found for N-BPs that exist only to a limited extent as their carbocation analogues at physiological pH, appears to be at variance with the currently held opinion that N-BPs inhibit FDP synthase primarily because they mimic carbocation transition state intermediates.[9] A deeper understanding of these results must await more detailed crystal-structure analysis of FDP synthase-ligand complexes.

Nitrogen-Containing Bisphosphonates and Inhibition of Growth of *Dictyostelium discoideum*. Previous investigations found that **7** is more potent than risedronate at inhibiting growth of *Dictyostelium* whereas **6**, which differs from **7** only by absence of a methyl group from the aromatic ring (Figure 1), is of a similar potency to risedronate.[4] However, **7** and **6** are about five- and three-fold less potent, respectively, than risedronate at inhibiting FDP synthase (Table 3). Nitrogen-containing bisphosphonates **7** and **6** also differ from risedronate by existing to a greater extent as carbocation analogues at physiological pH (Figure 4), and it is notable that **7**, which exists to a greater extent than **6** as the carbocation analogue, is the more potent inhibitor of growth of *Dictyostelium* despite its being the less potent FDP synthase inhibitor. Similarly, **3** and **5**, which exist almost entirely as carbocation analogues at physiological pH, are more potent as inhibitors of *Dictyostelium* growth than would have been expected from their relatively low potency as inhibitors of FDP synthase (Table 3). However, **2**, which, like risedronate, exists to only a small extent as the carbocation analogue at physiological pH (Figure 4b), and **1**, for which there is no carbocation form, appear to have potencies as inhibitors of *Dictyostelium* growth more in accord with their potencies as inhibitors of FDP synthase (Table 3).

The effect of an increasing microscopic pk_a for the nitrogen group in enhancing inhibition of growth of *Dictyostelium* amoebae by N-BPs differs from the effect of the pK_as of some pyridyl N-BPs tested on *Entamoeba histolytica*.[24] The apparent toxicity of the latter was found to correlate with diminishing pK_a although the quoted pyridyl pK_as were computed and not determined experimentally. This contrast may reflect differences between the mechanisms of uptake for N-BPs by *E. histolytica* and the Ax-2 strain of *Dictyostelium*.

Overall for *Dictyostelium*, it would appear that the existence of risedronate and its analogues in the carbocation form is *disadvantageous* to inhibition of FDP synthase while being *advantageous* to inhibition of amoebal growth. It is this disparity that results in the poor correlation between the potency of risedronate and its analogues as inhibitors of FDP synthase and as inhibitors of growth of *Dictyostelium*.

Effects of Nitrogen-Containing Bisphosphonates 8 and 9 and Alendronate. Nitrogen-containing bisphosphonate **9** is an analogue of risedronate that differs from the parent compound only by having an extra methylene group in the linker chain

between the pyridine ring and the bisphosphonate group (Figure 1). Nevertheless, this small difference in chemical structure is sufficient to cause a large change in biological properties since **9** is 24-fold less potent than risedronate at inhibiting growth of *Dictyostelium*[4] and is also considerably less potent than risedronate as an inhibitor of FDP synthase.[5] In the same way, **8** differs from **7** only by having an extra methylene group in the linker chain (Figure 1), but **8** remains a strong inhibitor of *Dictyostelium* growth[4] although, in common with **9**, it is an extremely poor inhibitor of FDP synthase (Table 3). The values of pK_a3 and pK_a4 for **9** (Table 1) are similar to those for risedronate so that **9** will resemble risedronate by existing to only a minor extent as the carbocation analogue at physiological pH. By contrast, the values of pK_a3 and pK_a4 for **8** (Table 1) indicate that it will resemble **7** and be present at physiological pH largely as the carbocation analogue. Thus it becomes possible to explain the difference[4] between the growth-inhibitory effects of **9** and **8** because only the latter can exist largely as the carbocation analogue at physiological pH which appears to be essential for potent inhibition of *Dictyostelium* growth by risedronate analogues that are relatively poor inhibitors of FDP synthase. The remarkable enhancement in the growth inhibitory effects of **8** is further evident when it is compared with **1** which is a similarly poor inhibitor of FDP synthase but also remains a poor inhibitor of *Dictyostelium* growth (Table 3) because it cannot exist as a carbocation analogue.

Although, initially, alendronate had been found to be only slightly less potent than risedronate as an inhibitor of *Dictyostelium* growth,[3] it was later shown to be at least 50-fold less potent than risedronate as an inhibitor of FDP synthase[5] (Table 3). The latter may now be rationalized because alendronate is present largely as the carbocation analogue at physiological pH. In addition, it is possible to account for the high potency of alendronate as an inhibitor of the growth of *Dictyostelium* because its predominant carbocation form will, as in the case of risedronate analogues that exist predominantly as the carbocation analogue at physiological pH, enhance inhibition of *Dictyostelium* growth by a mechanism that is not directly dependent on inhibition of FDP synthase.

Conclusions

Role of the Nitrogen Atom in Nitrogen-Containing Bisphosphonate Drugs. It is apparent that there must be two distinct roles for the essential nitrogen atom present in the N-BPs because there are two different and conflicting characteristics that the nitrogen atom needs to possess in order for the N-BPs to have high potency. First, potent inhibition of FDP synthase appears dependent on an uncharged nitrogen atom, but second, the overall biological effects of the N-BPs, as monitored by inhibition of *Dictyostelium* growth, are favored by a positively charged, protonated nitrogen. At the same time, the properties of the *D. discoideum* mutant strain RB 101 indicate that inhibition of *Dictyostelium* growth is always dependent to some extent on inhibition of FDP synthase. The mutant strain, originally selected for resistance to the growth inhibitory effects of risedronate, is also resistant to the growth inhibitory effects both of risedronate analogues and of other N-BPs owing to overproduction of FDP synthase.[5]

It might appear possible to account fully for the two different roles of the nitrogen atom in the N-BPs if, in addition to inhibiting FDP synthase, the N-BPs are taken up differentially by *Dictyostelium* amoebae or, owing to activity of a plasma membrane multidrug-resistance pump, are subject to selective efflux from amoebae, in either case, in a manner dependent on the charge associated with the nitrogen-containing group in the N-BPs. However, neither of these proposals appears probable. First, it has been shown that uptake of bisphosphonates by *Dictyostelium* amoebae growing in axenic culture is by macropinocytosis, and this is a nonselective process.[25,26] Second, the N-BPs lack structural features characteristic of substrates for plasma membrane multidrug-resistance pumps.[27] In particular, they are not lipophilic. Thus, in order to account for the overall effects of the N-BPs on *Dictyostelium*, it has to be concluded that they interact not only with FDP synthase but also with a second intracellular target. This has been confirmed by isolation of a mutant strain of *Dictyostelium* that neither overproduces FDP synthase nor contains an FDP synthase with aberrant properties but which, nonetheless, has resistance to the growth inhibitory effects of N-BPs.[28] Finally, because the rankings of the N-BPs in order of potency as inhibitors of osteoclast-mediated bone resorption and as inhibitors of *Dictyostelium* growth are so well-matched,[3,4] it would appear likely that there is also a second target for the N-BPs in osteoclasts and that the antiresorptive properties of the N-BPs are more complex than previously suspected.

Experimental Section

Bisphosphonates. Alendronate, risedronate, and the risedronate analogues **2**, **5**, **6** (NE 11807), **7** (NE 97220), **8** (NE 11809), and **9** (NE 58051) (Figure 1 and ref 4) were generously provided by Dr F. H. Ebetino, Procter & Gamble Pharmaceuticals, Cincinnati, OH, U.S.A. Tetraisopropyl methylenebisphosphonate was from Aldrich.

Tetraisopropyl 2-(3′-Pyridyl)-ethylidenebisphosphonate. Anhydrous toluene (100 mL) was added to toluene-washed potassium hydride (7.03 g, 58.5 mmol of a 35% suspension in oil) and stirred at 0 °C. Tetraisopropyl methylenebisphosphonate (10 g, 29 mmol) was added dropwise and the mixture stirred at rt for 1 h. 3-Picolyl chloride hydrochloride (5.69 g, 34.7 mmol) in dry DMSO (25 mL) was added dropwise to this solution at 0 °C and the dark brown mixture stirred at rt for 20 h. Anhydrous diethyl ether (100 mL) was added at 0 °C to precipitate potassium chloride, the reaction mixture filtered through Celite, and the filtrate taken up in KCl(aq) solution (50 mL, 50% saturated). The mixture was extracted with diethyl ether (6 × 50 mL), and the combined ether washings were dried over magnesium sulfate, filtered, and evaporated *in vacuo* to yield a dark brown viscous oil. Excess DMSO was removed in vacuo at 50 °C and the crude product purified by MPLC on silica gel (100% DCM to 10% EtOH in DCM gradient). The product was obtained as a viscous yellow oil (6.4 g, 51%). *m/z* (CI + ve) 436 ($M + H^+$), 393, 270, 186. δ_H ($CDCl_3$) 8.5−8.3 (2H, m, pyr); 7.6−7.5 (1 H, m, pyr); 7.2−7.1 (1 H, m, pyr); 4.8−4.6 (4 H, m, C*H*(Me)$_2$); 3.15 (2 H, td, $^3J_{PH} = 15$ Hz, $J = 6$ Hz, P_2CHCH_2); 2.4 (1 H, tt, $^2J_{PH}$ 24 Hz, $J = 6$ Hz, P_2CH); 1.3−1.1 (24 H, m, CH(*Me*)$_2$). δ_P ($CDCl_3$) 20.82 (s). δ_C ($CDCl_3$) 147 (py); 145 (py); 143 (py); 140 (py); 127 (py); 72 (*C*H(Me)$_2$); 39 (t, $J_{PC} = 132$ Hz, P_2CH); 29 (P_2CHCH_2); 24 (CH(*Me*)$_2$).

2-(3′-(*N*-Ethyl)pyridinium)-ethylidenebisphosphonic Acid (3). Tetraisopropyl 2-(3′-pyridyl)-ethylidenebisphosphonate (200 mg, 0.46 mmol) in dry acetonitrile (1.2 mL) and ethyl iodide (0.15 mL, 3 equiv) were stirred at rt for 5 min under argon. The reaction mixture was heated under reflux for 48 h and then evaporated to dryness in vacuo. The sticky brown residue was repeatedly triturated with anhydrous diethyl ether for 2 d and then with dry ethyl acetate for 1 d. Drying under high vacuum for a further day gave the tetraisopropyl ester iodide of the *title compound* as a hygroscopic white solid (266 mg, 98%). *m/z* (FAB + ve) 464 (M^+)(−I). δ_H (D_2O) 8.8−8.7 (2 H, m, py); 8.5−8.4 (1 H, m, py); 8.1−7.9 (1 H, m, py); 5.0−4.9 (2 H, m, N−CH_2); 4.8−4.6 (4 H, m, C*H*(Me)$_2$); 3.15 (2 H, td, $^3J_{PH} = 15$ Hz, $J = 6$ Hz, P_2CHCH_2); 2.4 (1 H, tt, $^2J_{PH} = 24$ Hz, $J = 6$ Hz, P_2CH); 1.6 (3 H, t, $J = 6$ Hz); 1.3−1.1 (24 H, m, CH(*Me*)$_2$). δ_P (D_2O) 20.6 (s). δ_C ($CDCl_3$) 147 (py); 145

(py); 143 (py); 140 (py); 127 (py); 72 (*C*H(Me)$_2$); 61 (*C*H$_2$); 39 (t, J_{PC} = 132 Hz, P$_2$*C*H); 30.1 (*C*H$_3$); 29 (P$_2$CH*C*H$_2$); 24 (CH(*Me*)$_2$).

The solid obtained from the above procedure was taken up in 6 M HCl (10 mL) and heated under reflux for 24 h under nitrogen. The clear yellow reaction mixture was evaporated to dryness in vacuo. Methanol (10 mL) was added, and the mixture again evaporated to dryness. This procedure was repeated three times, and then the brown gum was triturated with anhydrous diethyl ether to give the *title compound* as a sticky brown hygroscopic solid (108 mg, 79%). Titration of the solid with 1 M NaOH to pH 5 gave the disodium salt of the product as a light brown solid (results below are for free acid). HRMS (FAB + ve) $C_9H_{15}P_2O_6NNa$ requires 318.02724; found 318.02729. *m/z* (FAB + ve) 296 $(MH)^+$; 318 $(M + Na^+)$. δ_H (D_2O) 8.9−8.6 (2 H, m, py); 8.5−8.4 (1 H, m, py); 7.9−7.8 (1 H, m, py); 4.7−4.6 (2 H, m, N−C*H*$_2$); 3.5−3.2 (2 H, m, P$_2$CHC*H*$_2$); 2.7−2.5 (1 H, m, P$_2$C*H*); 1.6 (3 H, t, J = 6 Hz, C*H*$_3$). δ_P (D_2O) 19.9 (s). δ_C (D_2O) 145 (py); 144 (py); 143 (py); 141 (py); 126 (py); 59 (*C*H$_2$); 41 (P$_2$*C*); 31 (*C*H$_3$); 29 (P$_2$C*C*).

1-Hydroxy-2-(phenyl)-ethane-1,1-bisphosphonate (1). This was prepared from the reaction of phenylacetyl chloride (1 equiv) with tris-trimethylsilyl phosphite (2 equiv) at 25 °C and purified as previously described.[29] δ_P (D_2O) 19.0 (s).

2-(*N*-3″-Thiopropyl)-pyridinium-3′-yl)-ethylidenebisphosphonate (4). Tetraisopropyl 2-(3′-pyridyl)-ethylidenebisphosphonate (653 mg, 1.5 mmol) was treated with 3-bromopropyl thioacetate (600 mg, 3.0 mmol) in dry acetonitrile (10 mL) and heated under reflux for 20 h. The reaction mixture was cooled and evaporated and the gummy residue triturated with hexane and diethyl ether. Flash silica chromatography eluting with DCM:MeOH (4:1) gave tetraisopropyl 2-(3′-(*N*-3″-acetylthiopropyl)pyridinium)-ethylidenebisphosphonate bromide as a brown oil (768 mg, 1.2 mmol, 81%). *m/z* (FAB + ve) 552 (M+), δ_P 19.7 (s), δ_C($CDCl_3$) 195 (Me*C*O); 146 (py); 143 (py); 127 (py); 72, 71 (*C*HMe$_2$); 60 (*C*H$_2$); 39 (t, J_{PC} = 124.5 Hz, P$_2$*C*); 31 (*C*H$_2$); 30 (*C*H$_2$); 29 (P$_2$C*C*); 25 (*C*H$_2$); 24, 23 (CH(*C*H$_3$)$_2$). This ester was heated with HCl (6 M, 30 mL) under reflux for 36 h. After cooling and filtration, evaporation in vacuo gave a viscous yellow oil that was triturated with dry ether and dry ethyl acetate. Purification by MPLC on DEAE Sephadex using gradient elution with TEAB (0.1−0.4 M) and subsequent conversion of the tetrakis triethylammonium salt into the free acid (Amberlite IR 120H) and freeze-drying gave the product as a white hygroscopic solid (250 mg, 61%). Calcd for $C_{10}H_{17}NSO_6P_2 \cdot 4H_2O$: C, 29.06; H, 6.09; N, 3.40; S, 7.75. Found: C, 28.97; H, 5.59; N, 3.68; S, 7.19. *m/z* (ES + ve) 342 $(M + H^+)$. δ_H (D_2O) 8.8 (1 H, s, py); 8.7 (1 H, d, J = 7 Hz, py); 8.5 (1 H, d, J = 7 Hz, py); 8.0 − 7.9 (1 H, m, py); 4.7 (2 H, t, J = 6 Hz, C*H*$_2$N); 3.3 (1 H, s, S*H*); 3.4 (2 H, dt, J = 6 Hz, NCH$_2$C*H*$_2$); 2.7 (1 H, tt, J = 6 Hz, 22 Hz, P$_2$C*H*); 2.5 (2 H, t, J = 6 Hz, SC*H*$_2$); 2.4−2.2 (2 H, m, C*H*$_2$). δ_P (D_2O) 19.7 (s).

Potentiometric Titrations. Bisphosphonates were dissolved in 150 mM NaCl, and 4 mL samples, usually at 2.5 mM, were titrated by addition of 0.5 M KOH in 150 mM NaCl generally across the pH range 3−10 with aliquots added at rt by use of a Gilson P2 micropipette. A Hanna model 8519 pH meter and a BDH Gelplas combination pH electrode were used to follow changes in pH. The electrode was calibrated by use of buffers at pH 4.00 and pH 7.00 and the calibration checked with a buffer at pH 10.06 to an accuracy ≤0.05. Following potentiometric titrations, values for macroscopic pK_as were obtained by analysis of the plots of pH against the volume of KOH by use of a nonlinear fit package in Mathematica that employed an equation for a tetraprotic dissociation for risedronate, **6**, **7**, and **8** and a triprotic equation for **1**, **2**, **4**, **9**, and alendronate. In general, for the tetraprotic systems, pK_a2 was below 2 and was not well-determined by the program, but pK_a5 could be obtained for all N-BPs studied. The fits achieved have r^2 values greater than 0.992 and standard errors of less than 0.08 for pK_a3 and pK_a4.

Spectrophotometry. For determination of microconstants, 4 mL of 0.2 mM risedronate in 150 mM NaCl or 4 mL of 0.5 mM **2** in 150 mM NaCl were titrated with 0.5 M KOH in 150 mM NaCl. Changes in absorbance at 262 nm (risedronate) or at 283 nm (**2**) were measured in a Unicam Heλios γ spectrophotometer.

NMR Spectroscopy. Solutions of bisphosphonates were prepared at 20 mM (risedronate and **6**) or 10 mM (**7**) in 150 mM NaCl/10% (v/v) D_2O and were titrated with 4 M KOH in 150 mM NaCl. Samples were taken at measured pH values and examined by ^{1}H, ^{13}C, and ^{31}P NMR spectroscopy. ^{1}H, ^{31}P, and ^{13}C NMR spectra were run on a Bruker DRX 500 MHz spectrometer, utilizing a 5 mm BB probe, at 298 K, for 8, 128, and 512 scans respectively for risedronate and 8, 128, and 1024 scans respectively for **7**. For **6**, ^{1}H and ^{1}H−^{13}C (natural abundance) HSQC (standard Bruker pulse program) spectra were run on a Bruker Avance 800 MHz spectrometer with a 5 mm TXI probe, also at 298 K, to obtain ^{1}H and ^{13}C chemical shifts. The 1D spectra were acquired for 32 scans and the 2D HSQC for 8 scans and 400 data points in the second dimension, over a ^{13}C spectral width of 24150 Hz. Long-range HSQC spectra (utilizing $^2J_{CH}$ and $^3J_{CH}$) were run on some of the samples to check the assignment of ^{1}H and ^{13}C chemical shifts. Chemical shifts were referenced to internal DSS.

Substrates for Farnesyl Diphosphate Synthase. [4−^{14}C]-Isopentenyl pyrophosphate, triammonium salt, was obtained from NEN, Hounslow, U.K., and geranyl pyrophosphate, ammonium salt, from Sigma.

Specific Activity of Farnesyl Diphosphate Synthase. Amoebal extracts were prepared as previously described[5] with omission of the centrifugation step. The combined activities of FDP synthase and isopentenyl diphosphate isomerase were determined at 22 °C by use of geranyl pyrophosphate and [^{14}C]-isopentenyl pyrophosphate as substrates.[5] It had been shown previously that 100 nM risedronate completely inhibits the activity of FDP synthase but is without effect on isopentenyl diphosphate isomerase.[5] It was therefore possible to determine the activity of FDP synthase alone in the extracts as that portion of the combined activities of isopentenyl diphosphate isomerase and FDP synthase inhibited by 100 nM risedronate. Specific activity was calculated after the protein concentration in each extract had been determined by use of the Sigma Bradford Reagent with bovine serum albumin as the standard.

Growth of *Dictyostelium discoideum*. Amoebae of *D. discoideum* strain Ax-2 were grown axenically at 22 °C in HL5 glucose medium with shaking at 160 rpm.[30] Amoebal growth was monitored as described previously in 6 or 8 mL cultures maintained in six-well tissue culture plates.[3] Values of IC_{50} for inhibition of *Dictyostelium* growth by N-BPs were determined from growth curves.[3,4] IC_{50} has been defined as the concentration of a bisphosphonate that allows only half the number of cell divisions that would have occurred in the absence of the bisphosphonate.[3,4]

Acknowledgment. We thank the Wellcome Trust for financial support (to D.R.), Procter & Gamble for a grant (to J.C.), and the National Association for the Relief of Paget's Disease for award of the Ann Stansfield Fellowship to R.J.B. We are also grateful for help from Prof. M. J. Hounslow in programming the model for NMR−pH titration analysis and speciation and for helpful discussions with Prof. J. P. Waltho.

Supporting Information Available: Figures S1, S2, and S3 showing the NMR−pH titration data and curve fits for risedronate, **6** and **7**, respectively. Figure S4 showing potentiometric titration data and curve fits for all compounds listed in Table 1. Equations for fitting potentiometric titration data. This material is available free of charge via the Internet at http://pubs.acs.org.

References

(1) Fleisch, H. *Bisphosphonates in Bone Disease. From Laboratory to the Patient*; The Parthenon Publishing Company: New York and London, 1995.
(2) Russell, R. G. G. Bisphosphonates. From bench to bedside. *Ann. N.Y. Acad. Sci.* **2006**, *1068*, 367–401.
(3) Rogers, M. J.; Watts, D. J.; Russell, R. G. G.; Ji, X.; Xiong, X.; Blackburn, G. M.; Bayless, A. V.; Ebetino, F. H. Inhibitory effects of bisphosphonates on growth of amoebae of the cellular slime mold Dictyostelium discoideum. *J. Bone Miner. Res.* **1994**, *9*, 1029–1039.

(4) Rogers, M. J.; Xiong, X.; Brown, R. J.; Watts, D. J.; Russell, R. G. G.; Bayless, A. V.; Ebetino, F. H. Structure-activity relationships of new heterocycle-containing bisphosphonates as inhibitors of bone resorption and as inhibitors of growth of Dictyostelium discoideum amoebae. *Mol. Pharmacol.* **1995**, *47*, 398–402.
(5) Grove, J. E.; Brown, R. J.; Watts, D. J. The intracellular target for the antiresorptive aminobisphosphonate drugs in Dictyostelium discoideum is the enzyme farnesyl diphosphate synthase. *J. Bone Miner. Res.* **2000**, *15*, 971–981.
(6) Schenk, R.; Eggli, P.; Fleisch, H.; Rosini, S. Quantitative morphometric evaluation of the inhibitory activity of new aminobisphosphonates on bone resorption in the rat. *Calcif. Tissue Int.* **1986**, *38*, 342–349.
(7) Sietsema, W. K.; Ebetino, F. H.; Salvagno, A. M.; Bevan, J. A. Antiresorptive dose-response relationships across three generations of bisphosphonates. *Drugs Exp. Clin. Res.* **1989**, *15*, 389–396.
(8) Martin, M. B.; Arnold, W.; Heath, H. T.; Urbina, J. A.; Oldfield, E. Nitrogen-containing bisphosphonates as carbocation transition state analogs for isoprenoid biosynthesis. *Biochem. Biophys. Res. Commun.* **1999**, *263*, 754–758.
(9) Poulter, C. D.; Rilling, H. C. The prenyl transfer reaction. Enzymatic and mechanistic studies of the 1′-4 coupling reaction in the terpene biosynthetic pathway. *Acc. Chem. Res.* **1978**, *11*, 307–313.
(10) Tarshis, L. C.; Yan, M.; Poulter, D.; Sacchettini, J. C. Crystal structure of recombinant farnesyl diphosphate synthase at 2.6-Å resolution. *Biochemistry* **1994**, *33*, 10871–10877.
(11) Hosfield, D. J.; Zhang, Y.; Dougan, D. R.; Broun, A.; Tari, L. W.; Swanson, R. V. Structural basis for bisphosphonate-mediated inhibition of isoprenoid biosynthesis. *J. Biol. Chem.* **2004**, *279*, 8526–8529.
(12) Rabenstein, D. L. Nuclear magnetic resonance studies of the acid-base chemistry of amino acids and peptides. 1. Microscopic ionisation constants of glutathione and methylmercury-complexed glutathione. *J. Am. Chem. Soc.* **1973**, *95*, 2797–2803.
(13) Ebrahimpour, A.; Ebetino, F. H.; Sethuraman, G.; Nancollas, G. H. Determination of solubility and calcium ion stability constants of a phosphonoalkylphosphinate (PAP) and bisphosphonates (BPs) such as EHDP, risedronate, alendronate, 3-pic AMBP, and 3-pic AMPMP. In *Mineral scale formation and inhibition*; Amjad, Z., Ed.; Plenum Press: New York, 1995; pp 295−305.
(14) Szakács, Z.; Kraszni, M.; Noszál, B. Determination of microscopic acid-base parameters from NMR-pH titrations. *Anal. Bioanal. Chem.* **2004**, *378*, 1428–1448.
(15) Breitmaier, E.; Spohn, K.-H. P_H-abhängigkeit der ^{13}C-chemischen verschiebungen sechsgliedriger stickstoff-heteraromaten. *Tetrahedron* **1973**, *29*, 1145–1152.
(16) Perrins, D. D. *Dissociation constants of organic bases in aqueous solution*; Butterworths: London, 1965; p 145.
(17) Jencks, W. P.; Regenstein, J. Ionization constants of acids and bases. In *Handbook of biochemistry and molecular biology*; Fasman, G. D., Ed.; CRC Press: Cleveland, OH, 1976; Vol. 1, pp 305−351.
(18) Hägele, G.; Szakács, Z.; Ollig, J.; Hermens, S.; Pfaff, C. NMR-controlled titration: characterizing aminophosphonates and related structures. *Heteroat. Chem.* **2000**, *11*, 526–582.
(19) Boduszek, B.; Dyba, M.; Jezowska-Bojczuk, M.; Kiss, T.; Kozlowski, H. Biologically active pyridine mono- and bis-phosphonates: efficient ligands for co-ordination of Cu^{2+} ions. *J. Chem. Soc., Dalton Trans.* **1997**, 973–976.
(20) Matczak-Jon, E.; Sowka-Dobrowolska, W.; Kafarski, P.; Videnova-Adrabinska, V. Molecular organisation and solution properties of N-substituted aminomethane-1,1-diphosphonic acids. *New J. Chem.* **2001**, *25*, 1447–1457.
(21) Ullman, G. M. Relations between protonation constants and titration curves in polyprotic acids: A critical view. *J. Phys. Chem. B* **2003**, *107*, 1263–1271.
(22) Hägele et al.[18] sought to use ^{31}P NMR to identify microscopic pk_a values for three nitrogen-containing bisphosphonates but failed to allow for the titration of water at extremes of pH, thereby making their results somewhat unreliable.
(23) Insufficient material was available for these determinations.
(24) Ghosh, S.; Chan, J. M. W.; Lea, C. R.; Meints, G. A.; Lewis, J. C.; Tovian, Z. S.; Flessner, R. M.; Loftus, T. C.; Bruchhaus, I.; Kendrick, H.; Croft, S. L.; Kemp, R. G.; Kobayshi, S.; Nozaki, T.; Oldfield, E. Effects of bisphosphonates on the growth of Entamoeba histolytica and Plasmodium species in vitro and in vivo. *J. Med. Chem.* **2004**, *47*, 175–187.
(25) Rogers, M. J.; Xiong, X.; Ji, X.; Mönkkönen, J.; Russell, R. G. G.; Williamson, M. P.; Ebetino, F. H.; Watts, D. J. Inhibition of growth of Dictyostelium discoideum amoebae by bisphosphonate drugs is dependent on cellular uptake. *Pharm. Res.* **1997**, *14*, 625–630.
(26) Maniak, M. Macropinocytosis. In *Endocytosis*; Marsh, M., Ed.; Oxford University Press: Oxford, 2001; pp 78−93.
(27) Seelig, A. A general pattern for substrate recognition by P-glycoprotein. *Eur. J. Biochem.* **1998**, *251*, 252–261.
(28) Watts, D. J. Unpublished results.
(29) Lecouvey, M.; Mallard, I.; Bailly, T.; Burgada, R.; Leroux, Y. A mild and efficient one-pot synthesis of 1-hydroxymethylene-1,1-bisphosphonic acids. *Tetrahedron Lett.* **2001**, *42*, 8475–8478.
(30) Watts, D. J.; Ashworth, J. M. Growth of myxamoebae of the cellular slime mould Dictyostelium discoideum in axenic culture. *Biochem. J.* **1970**, *119*, 171–174.

JM7015792